RAPID COMMUNICATIONS

PHYSICAL REVIEW C VOLUME 47, NUMBER 5 MAY 1993

Significance of inclusive electron-nucleus cross sections ratios in the multi-GeV region

S. Liuti*

Institute of Nuclear and Particle Physics, University of Virginia, Charlottesville, Virginia 22901

(Received 14 July 1992)

Ratios of inclusive electron-nucleus cross sections are studied at incoming electron energies of 1 GeV to 25 GeV and (Bjorken) variable $x_{\rm Bj} > 1$ where many of the present theoretical speculations and the available and forthcoming experimental data are focused on. An alternative analysis which accounts for nuclear target mass effects is proposed.

PACS number(s): 25.30.−C

In the past few years inclusive lepton-nucleus scattering in the region between a few GeV and a few tens of GeV for the initial lepton energy (the multi-GeV region) has acquired a growing importance as a means for investigating hadronic systems. The interest in such a kinematical region is in that it represents an atypical domain for studying the structure of nucleons and nuclei, where nonstandard nuclear configurations other than meson and nucleon degrees of freedom (e.g., few-nucleon correlations or multiquark clusters) should play a relevant role, where constituent quarks are replaced by current quarks, and where perturbative QCD makes a transition to nonperturbative QCD. In order to clearly identify the contribution of different degrees of freedom, it is useful to consider kinematical regions where one hadronic configuration is supposed to become dominant over the other ones. To this end in this paper we concentrate on the region of (Bjorken) $x_{\rm Bj} > 1$ where scattering off a stationary nucleon is forbidden and the contribution of high momentum components in nuclei, such as few-nucleon correlations or other exotic configurations, can be more easily singled out. A clear understanding of the contribution of different degrees of freedom at $x_{\rm Bj} > 1$ would help solve the "puzzle" of the original EMC effect [1]. Available inclusive data at $x_{\rm Bj} > 1$ have been plotted in the form of ratios of cross sections for heavy nuclei to the ones for lighter nuclear systems such as deuteron [2] and ^{4}He [3]. In particular, at the kinematics of [3], which corresponds to average four-momentum squared $\langle Q^2 \rangle \approx 1 - 3\,{\rm GeV}^2$, data seem to exhibit plateaus, i.e., a constant behavior of the ratios as a function of $x_{\rm Bj}$, for values of $x_{\rm Bj} \geq 1.2$. Such a behavior is not found in [2], where data extend up to $x_{\rm Bj} \approx 1.3$ and $\langle Q^2 \rangle \leq 4\,{\rm GeV}^2$. Plateaus in inclusive cross sections ratios have been originally predicted by Vary *et al.* [4] within the *multiquark* cluster model. According to [4], ratios of heavier to lighter nuclei should show a staircase behavior, the width of each step being $n-1 < x_{\rm Bj} < n$, for integer $n \geq 2$, and the height of each step being proportional to the ratios of probabilities of the dominant multiquark configuration in the heavier and in the lighter nucleus, respectively. Similarly, Frankfurt and Strikman [5] suggested that within the *few-nucleon correlation* model, the height of the plateau which appears in the data for $1 < x_{\rm Bj} < 2$ should be related to the probability for the onset of the dominant few-nucleon configuration (in this case the two-nucleon correlation).

Our analysis is aimed at clarifying by means of quantitative calculations the following points: (1) Correlations are believed to account for the phenomenology of the short-distance structure of nuclei. High momentum components cannot be completely isolated at $x_{\rm Bj} > 1$ and $Q^2 \leq 15\,{\rm GeV}^2$ due to a persisting contribution of the low momentum and energy nuclear structure; (2) nuclear *target mass effects* which are remarkably different, e.g., in a complex nucleus and in a deuteron are important in the evaluation of cross sections ratios for different nuclei and if not taken into account (as done, e.g., in [2,3] and [4,5]) they lead one to compare different ranges of momentum and energy components in the two nuclei. A clear understanding of possible recurrences of correlations (particularly in the form of plateaus) is therefore hindered and as a possible remedy, we propose an analysis in terms of alternative scaling variables. Both a careful evaluation of different nuclear components and the change in scaling variables that we propose define a substantially different method of analyzing and interpreting experimental data at $x_{\rm Bj} > 1$ compared with [2,3] and [4,5], respectively. We show that the extension of such a method at $x_{\rm Bj} > 1$ and higher Q^2 ($Q^2 \approx 20\ {\rm GeV}^2$) gives results that largely differ from previous approaches. We conclude that it would be of primary importance to consider points (1) and (2) in the analysis of the new set of experiments proposed in [6], with the aim of eventually singling out in a clear-cut way the contribution of novel features of the short-distance structure of nuclei.

In the (plane wave) impulse approximation (IA) the inclusive cross section for electron scattering by a nucleus A is given by

$$\sigma_A \equiv \frac{d^2\sigma}{d\Omega_{e'}\,d\epsilon_2} = \sigma_{\rm Mott}[W_2^A(Q^2,\nu) + 2\tan^2(\theta/2)W_1^A(Q^2,\nu)], \quad (1)$$

where $\sigma_{\rm Mott} = \alpha^2 \cos^2\frac{\theta}{2}/4\epsilon_1^2 \sin^4\frac{\theta}{2}$ is the Mott cross section, ϵ_1 and ϵ_2 are the incoming and outgoing electron energies, respectively, Q^2 is the squared four-momentum transfer, $\nu = \epsilon_1 - \epsilon_2$ is the energy transfer, and θ is the scattering angle. Within IA, the nuclear responses $W_{1(2)}^A$ are written in terms as

*Permanent address: INFN, Sezione Sanita', Viale Regina Elena 299, I-00161, Roma, Italy.

$$W^A_{1(2)}(Q^2,\nu) = \int d^4k\, Z\, S(k)[C_{1(2)}W^p_1(Q^2,(kq),k^2) + D_{1(2)}W^p_2(Q^2,(kq),k^2)] + (\text{similar terms for neutrons}), \quad (2)$$

where $k \equiv (\mathbf{k}, k_0)$ is the struck nucleon's four-momentum, Z is the number of protons, $W^{p(n)}_{1(2)}$ are the off-shell proton (neutron) structure functions, $S(k)$ is the covariant vertex function at the $A \to (A-1)+N$ vertex, and $C_{1(2)}$ and $D_{1(2)}$ are kinematical factors determined by the choice of the off-shellness extrapolation for the free nucleon structure functions (see [12] for details). Equations (1) and (2) describe both quasielastic (qe) nucleon knock-out and inelastic scattering. One selects either process through the structure functions $W^{N,\text{off}}_{1(2)}$, which can be chosen to represent either the elastic or the inelastic response of an off-shell nucleon. Such quantities cannot be related to the free nucleon structure functions in a model independent way and they appear to be modified in the nuclear medium (see, e.g., [7] for qe scattering and [8] for deep inelastic scattering). Although a fully consistent treatment of off-shell effects can be found, e.g., in [7], in this paper we adopt the *ad hoc* prescriptions of [9] and [10] for qe and inelastic scattering, respectively, in order to have an unbiased comparison with previous calculations which used the same prescriptions. We consider two ranges of Q^2 values at $x_{\text{Bj}} > 1$: the *intermediate* Q^2 region ($1 \le Q^2 \le 8\,\text{GeV}^2$ [2,3]) and the *high* Q^2 region ($Q^2 \gtrsim 20\,\text{GeV}^2$). In the intermediate region qe scattering dominates over the $x_{\text{Bj}} > 1$ tail of the inelastic cross section as proven, for instance, by the lack of large y-scaling violations in the experimental data [3]. In the high Q^2 region the nucleon elastic form factors suppress the qe cross section, allowing for a dominance of inelastic scattering, which is present at $x_{\text{Bj}} > 1$ proportionally to the amount of high momentum components in the target nucleus, and has a weak Q^2 dependence. A quantitative determination of such a pattern is model dependent, and there will always exist a range of Q^2 in which neither process dominates. Our calculations indicate that in order to suppress almost completely qe scattering, one needs $Q^2 \gtrsim 20\ \text{GeV}^2$.

In order to evaluate Eq.(2), the vertex function $S(k)$ is approximated [11] by the nonrelativistic spectral function

$$P^N(|\,\mathbf{k}\,|,E) = (2\pi)^{-3}\sum_f |\,\Phi_f(\mathbf{k})\,|^2\,\delta(E-(E^f_{A-1}-E_A)), \quad (3)$$

where $\Phi_f(\mathbf{k})$ is the Fourier transform of the overlap integral between the target nucleus A and the final $A-1$ system wave functions; E is the nucleon removal energy which is related to k_0 by: $k_0 = M_N - E - (\mathbf{k}^2/2M_{A-1})$; E_A and E^f_{A-1} are the total energies of the nucleus A and of the final $A-1$ system, respectively. $P^N(k,E)$ represents the joint probability that, after a nucleon with momentum k ($|\,\mathbf{k}\,| \equiv k$) has been removed from the target, the $(A-1)$ system is left with excitation energy $E^{f*}_{A-1} \equiv E^f_{A-1} - (M_{A-1} + M_N - M_A)$ (see [12] for details). The bulk of the effects of correlations, characterizing the short-distance part of the nucleon-nucleon interaction, is expected to have its largest impact on the high k and E components of the spectral function. This is precisely what different microscopic calculations show in the case of few-body systems ([12] and references therein) and nuclear matter [13]. Particularly, in [13] it was shown that $P^N(k,E)$ can be separated into a *single-particle* component which describes two-body breakup processes with the $A-1$ system recoiling coherently [$A \to (A-1)+N$], and a *background* component entirely generated by nucleon correlations and associated with multibody breakup processes [$A \to (A-2)+N+N, A \to (A-3)+N+2N, \ldots$]. For complex nuclei the spectral function cannot be calculated within a rigorous microscopic approach and it is necessary to construct a reasonable dynamical model which would account also for the high k and E components. To this end, we consider the following representation [12,14]

$$P^N(k,E) = P_0(k,E) + P_1(k,E), \quad (4)$$

where P_0 and P_1 represent the analogous of the single-particle and background components of nuclear matter [13], respectively. Here P_0 is calculated by approximating the microscopic calculation of the one-hole excitations in [13] with $P_0(k,E) = \sum_\alpha (A_\alpha/A) n_\alpha(k)\delta(E-|\,\epsilon_\alpha\,|)$, where $n_\alpha(k)$ is the momentum distribution of the single-particle state α associated with a Hamiltonian mean-field with single-particle energy ϵ_α and nucleon number A_α. Since correlations create states above the Fermi surface, they affect P_0 by reducing its overall strength with respect to mean-field descriptions. P_1 can be calculated according to the model of [11] where high momentum and energy components are described by configurations (*few-nucleon correlations*) in which two nucleons (or a cluster of nucleons) are found at a very small relative distance and are recoiling against each other with high k and E. Correlations are entirely responsible for the existence of inclusive scattering at $x_{\text{Bj}} > 1$. However, we now show

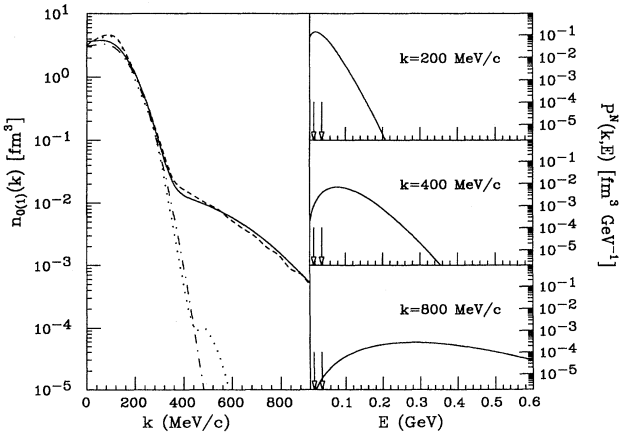

FIG. 1. (Left panel) n_0 (dot-dashes) and $n_0 + n_1$ (full) for ^{12}C. Shown for comparison are the results adapted from [15] for ^{16}O (dots and short dashes, respectively). (Right panel) P_1 for ^{12}C, Eq. (4), as a function of E for different values of k. Arrows indicate the position of the hole state energies, ϵ_α (see text).

P_1. $P_{o(1)}$ are constructed so as to satisfy the sum rules: $\int dE P_{0(1)}(k,E) = n_{0(1)}(k)$, where $n_0(k)$ and $n_1(k)$ are identified with the hole-state (microscopically calculated) momentum distribution and with the distribution of nucleons belonging to a correlation, respectively. $n_{0(1)}(k)$ used in our model are in good agreement with those obtained from highly accurate microscopic calculations for complex nuclei [15]. In Fig. 1 (left panel) we show the momentum distributions that we used for ^{12}C and compare them with the ones from Ref. [15] for ^{16}O. Notice that $n_0 \ll n_1$, for $k \geq k_M \approx 500$ MeV. In Fig. 1 (right panel) we show the E dependence of P_1 at different values of k. We also show the position of the hole states energies, ϵ_α ($\alpha = 1s, 1p$), where the components of P_0 are centered. Similar results are obtained for other nuclei. It is evident that in order to have P_0 and P_1 not interfering with each other one has to probe the high k and E region. The question of quantitatively determining at what values such a region can be found is still open and model dependent. We find as lower limiting values $k_M \approx 500$ MeV and $E_M \geq 100$ MeV, for all nuclei considered. One hopes [4,5] that a separation as the one in Eq. (4) can be seen experimentally by studying that this is not the case at intermediate Q^2, by quantitatively evaluating the contributions of P_0 and P_1 to inclusive cross sections ratios. Our results are given in Fig. 2 where we plot the ratios: $R_d = \sigma_A/\sigma_d$, of ^{4}He, ^{12}C, ^{27}Al, and ^{56}Fe to deuteron (d), $R_{\rm He} = \sigma_A/\sigma_{\rm He}$, of ^{56}Fe to ^{4}He, and $R_{\rm C} = \sigma_A/\sigma_{\rm C}$, of ^{56}Fe to ^{12}C. The most striking result that we obtain is the presence of a bump in the ratios R_d and $R_{\rm He}$, which shows that P_0 contributes substantially even at high $x_{\rm Bj}$. An analogous behavior is only slightly noticeable in the ratio $R_{\rm C}$ (Fig. 2, bottom), because the two-body breakup part of the spectral function, P_0, is similar in the two nuclear systems (^{56}Fe and ^{12}C). Therefore, by plotting ratios at $x_{\rm Bj} > 1$ and Q^2 of a few GeV^2, one cannot draw any significant conclusion concerning correlations.

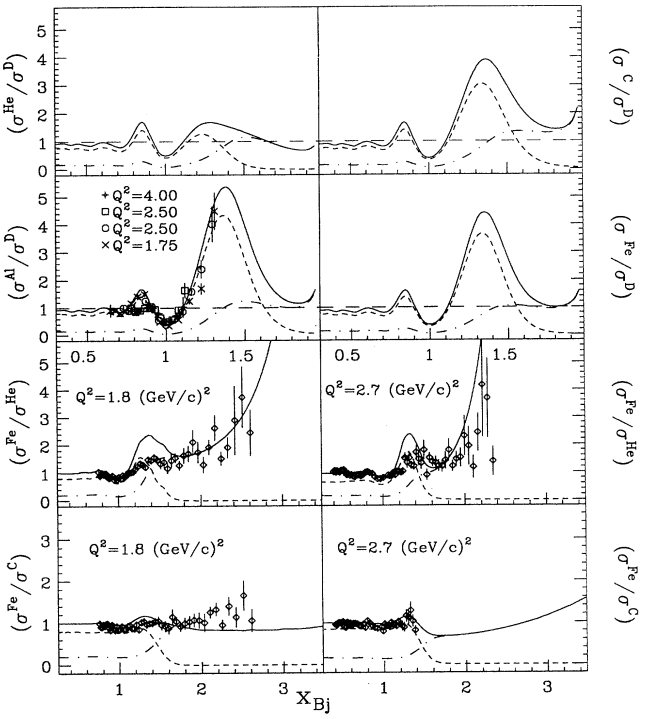

FIG. 2. Ratios of inclusive electron-nucleus cross sections per nucleon for ^{4}He, ^{12}C, ^{27}Al, and ^{56}Fe to deuteron (R_d in the text); for ^{56}Fe to ^{4}He ($R_{\rm He}$); and for ^{56}Fe to ^{12}C (R_C). Results are plotted vs $x_{\rm Bj}$, at $\theta = 15°$ and $\epsilon_1 = 5.5$ GeV ($\langle Q^2 \rangle = 1.75$ GeV^2) (R_d); at $\theta = 25°$ and $\epsilon_1 = 3.6$ GeV ($\langle Q^2 \rangle = 1.8$ GeV^2) (left); and at $\theta = 30°$ and $\epsilon_1 = 3.6$ GeV ($\langle Q^2 \rangle = 2.7$ GeV^2) (right) ($R_{\rm He}$ and $R_{\rm C}$). The short-dashed line is obtained by setting $P^N(k,E) \equiv P_0^N(k,E)$ in Eq. (9), the dot-dashed line corresponds to $P^N(k,E) \equiv P_1^N(k,E)$; and the full line is obtained when the entire spectral function [Eq. (4)] is considered. Experimental data for $\sigma_{\rm Al}/\sigma_d$ are from [2], data for $R_{\rm He}$ and $R_{\rm C}$ are from [3].

An even more important point is that by taking ratios at the same $x_{\rm Bj}$ one does not match the same regions in k and E of the two nuclei, thus spoiling previous interpretations in terms of plateaus. A possible remedy to such a situation is to describe data in terms of the y scaling variable [16] instead of $x_{\rm Bj}$. The necessary conditions for y scaling of nuclear structure functions are the validity of the IA and the assumption that the scattering process involves only nucleon degrees of freedom. In this paper we adopt a variable introduced in [17], which differs from the original one [16] in that it is derived without making nonrelativistic extrapolations in the kinematics. For a nucleus with mass M_A it reads

$$y_A = \{-|\mathbf{q}|[M_A^{*2} + M_{A-1}^2 - M_N^2] + (\nu + M_A)\sqrt{[M_A^{*2} + M_{A-1}^2 - M_N^2]^2 - 4M_A^{*2}M_{A-1}^2}\}/2M_A^{*2}, \quad (5)$$

where $M_A^{*2} = (\nu + M_A)^2 - \mathbf{q}^2$, M_{A-1} is the mass of the recoiling $A-1$ system, and $\mathbf{q}$ is the three-momentum transfer. In Eq. (5) we use the subscript A in order to underline the fact that y_A is different for different nuclear systems. When $M_{A-1}^2 \gg k^2$, i.e., when recoil of the $A-1$ system can be disregarded, such a variable becomes

$$y = -|\mathbf{q}| + \sqrt{(\nu - E_0)^2 + 2M_N(\nu - E_0)}, \quad (6)$$

E_0 being the minimum value of the removal energy. The relationship between y_A and y is analogous to that between Nachtmann ξ and $x_{\rm Bj}$. For $|\mathbf{q}| \to \infty$, y_A and y are related to the light-cone momentum fraction $z = (k^+/P_A^+)(M_A/M_N)$ carried by nucleons inside the nucleus by

$$y_A \equiv \frac{(M_A - zM_N)^2 - M_{A-1}^2}{2(M_A - zM_N)}, \quad y \equiv M_N(1-z) - E_0. \quad (7)$$

Equation (7) holds for qe scattering only. In inelastic scattering y is no longer related to k^+ or z [the energy conservation law from which Eq. (7) was derived becomes in this case a function of the invariant mass, of the final hadrons], but it can be generally related to $x_{\rm Bj}$ and Q^2:

$$y_A = \{-(Q^2/2M_N x_{\rm Bj})\sqrt{1+4M_N^2 x_{\rm Bj}^2/Q^2}[M_A^{*2}(x_{\rm Bj},Q^2)+M_{A-1}^2-M_N^2] + (Q^2/2M_N x_{\rm Bj}+M_A)\sqrt{[M_A^{*2}(x_{\rm Bj},Q^2)+M_{A-1}^2-M_N^2]^2-4M_A^{*2}(x_{\rm Bj},Q^2)M_{A-1}^2}\}/2M_A^{*2}(x_{\rm Bj},Q^2), \quad (8)$$

where $M_A^{*2}(x_{\rm Bj},Q^2) = M_A^2 + Q^2(\frac{M_A}{M_N x}-1)$. Consequently, one can always write W_2^A in Eq. (2) as a function of y_A and Q^2

$$W_2^A(y_A,Q^2) = 2\pi Z \int_{W_{\rm min}}^{W_{\rm max}(y_A,|\mathbf{q}|)} dW' W_2^p(Q^2,W') \int_{E_{\rm min}}^{E_{\rm max}(W',y_A,|\mathbf{q}|)} dE \times \int_{k_{\rm min}(y_A,|\mathbf{q}|,W',E)}^{k_{\rm max}(y_A,|\mathbf{q}|,W',E)} dk\, J(W',|\,\mathbf{q}\,|,k,E) D_2\, k\, P^p(k,E) + (\text{similar terms for neutrons}), \quad (9)$$

where $W' = \sqrt{(k+q)^2}$ is the invariant mass at the nucleon vertex, $J(W',|\mathbf{q}|,k,E) = [M_{A-1} + (E - E_{\rm min})]/\sqrt{M_{A-1}^2+k^2} \times (W'/\,|\,\mathbf{q}\,|)$ is the Jacobian of the transformation, and $C_2 = 0$. A similar expression holds for W_1^A. The integration limits in Eq. (9) are

$$W_{\rm min} = W_{\rm thr}, \quad W_{\rm max} = |\, M_A^* - M_{A-1}\,|, \quad (10a)$$

$$E_{\rm min} = M_N + M_{A-1} - M_A, \quad (10b)$$

$$E_{\rm max} = E_{\rm min} - M_{A-1} + |\, M_A^* - W'\,|,$$

$$k_{\rm min(max)} = \{-(+)\,|\,\mathbf{q}\,|[M_A^{*2}+M_{A-1}^2-W'^2] + (\nu+M_A)\sqrt{[M_A^{*2}+M_{A-1}^2-W'^2]^2-4M_A^{*2}M_{A-1}^2}\}/2M_A^{*2}, \quad (10c)$$

where $M_A^* = M_A^*(\nu,|\,\mathbf{q}\,|)$ and where $\nu = \nu(y_A,|\,\mathbf{q}\,|)$ is obtained by solving Eq. (5). Here, $W_{\rm thr} = M_N + m_\pi$ for inelastic scattering and $W_{\rm thr} = M_N$ for qe scattering. It is clear that at given $x_{\rm Bj}$ and Q^2, the values of the integration limits (10a)–(10c) for two nuclei A_1 and A_2 differ from each other because of the explicit dependence of Eqs. (10a)–(10c) on nuclear masses. As a result, at given $x_{\rm Bj}$ and Q^2, different ranges of the nucleon momentum and removal energy contribute to $W_2^{A_1}$ and $W_2^{A_2}$, respectively. Hence, contrary to what has been done so far, in order to study the recurrence of a given dynamical component in two different nuclei, one should compare the numerator and denominator of their cross sections ratios (R_d, ...) at values of $x_{\rm Bj}$ which differ from each other but which are chosen so as to give the same values for the integration limits (10a)–(10c), i.e., the same range in k and E in $P^N(k,E)$ [Eq. (4)]. Quantitatively such a procedure is accomplished by translating the mass dependence of the limits (10a)–(10c) into that of the variable y_A, in terms of which one writes the nuclear structure functions [Eq. (9)]: from the definition of y_A, Eq. (8), it follows that one probes the same dynamical components in A_1 and A_2, by taking their cross sections ratios at $y_{A_1} = y_{A_2}$ (and shifted $x_{\rm Bj}$). In Table I we demonstrate the numerical relevance of our prescription by comparing values of y_A for different nuclei at the same $x_{\rm Bj}$ and Q^2. The differences shown in Table I are significant if one takes into account the fact that W_2^A is a *rapidly varying* function of y_A [14]. Note also the difference with the variable y, Eq. (6), which is related in a unique way to $x_{\rm Bj}$ [18]. In Fig. 3 we show the ratios $R_d = \sigma_A(y_A = y_d)/\sigma_d(y_A = y_d)$, evaluated by fixing the value of $x_{\rm Bj}$ in the numerator and by calculating the denominator at a shifted value, $x_{\rm Bj} \to x_{\rm Bj} + \bar{x}$, so as to obtain the equality $y_A = y_d$. Notice that we still find a bump at $1 < x_{\rm Bj} < 1.5$ because such a feature mainly reflects the difference in the low k and E parts of P^N for complex nuclei and deuteron,

TABLE I. The scaling variable y_A in GeV, Eq. (8), at fixed $x_{\rm Bj}$ and $Q^2 = 3\ {\rm GeV}^2$, for deuteron (d), ^{4}He, ^{12}C, ^{27}Al, and ^{56}Fe. The differences found among all nuclei are numerically significant in regions where the nuclear structure functions, Eq. (9), varies rapidly with y_A.

$x_{\rm Bj}$	y_d	$y_{(^4{\rm He})}$	$y_{(^{12}{\rm C})}$	$y_{(^{27}{\rm Al})}$	$y_{(^{56}{\rm Fe})}$
1	-0.003	-0.023	-0.029	-0.014	-0.014
1.2	-0.131	-0.144	-0.148	-0.125	-0.124
1.4	-0.244	-0.240	-0.239	-0.221	-0.220
1.6	-0.374	-0.333	-0.323	-0.303	-0.301
1.8	-0.528	-0.416	-0.396	-0.373	-0.371

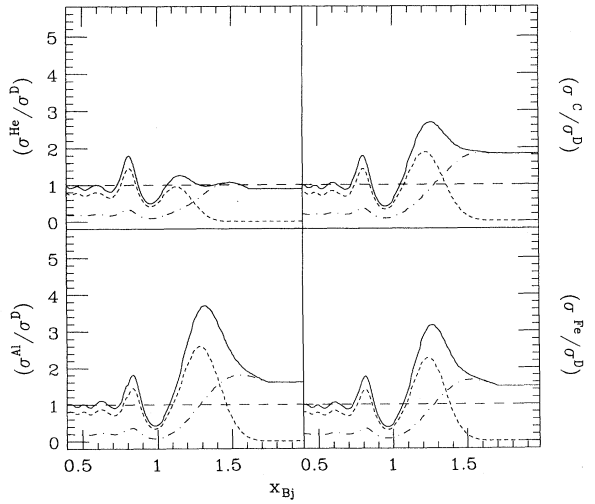

FIG. 3. Cross sections ratios for ^{4}He, ^{12}C, ^{27}Al, and ^{56}Fe to deuteron, plotted vs $x_{\rm Bj}$ and calculated by using the prescription $y_A = y_d$ explained in the text. Notations are as in Fig. 2.

respectively, and it does not depend significantly on the choice of scaling variables (see row 2 in Table I).

A more detailed study at intermediate Q^2 values would involve both final state interaction (FSI) and off-shell effects [19]. Although such a question is beyond the scope of this paper, it appears to us that FSI and off-shell effects would affect scattering from heavier and lighter nuclei in different amounts and consequently modify their cross section ratios. Any feature (including plateaus) in the high $x_{\rm Bj}$ and low Q^2 region would result from few concurring mechanisms, and prevent furthermore a direct study of high momentum components in nuclei. At high Q^2 contributions of FSI and nucleon off-shellness should become less important (see, e.g., [20]). Moreover, at $Q^2 \gtrsim 20\ \mathrm{GeV}^2$, where our estimates indicate that the contribution of qe scattering is highly suppressed, Eqs. (8)–(10) can be extrapolated to the Bjorken limit (Q^2, $\nu \to \infty$, $x_{\rm Bj}$ fixed) and an exact relationship between the values of $x_{\rm Bj}$ that yield the same value of y_A in two nuclei of different mass can be worked out. For a nucleus with $A > 12$, one obtains $y_A \approx y_d$ by substituting in the deuteron structure function: $x_{\rm Bj} \to x_{\rm Bj} + 1 - \sqrt{1 + (1 - x_{\rm Bj} - \langle E\rangle/M_N)^2 + (\langle E\rangle - E_d)/M_N}$, $\langle E\rangle$ being the average value of the removal energy in the nucleus A and E_d being the binding energy of deuteron. The ratios σ_A/σ_d for ^{56}Fe are shown in Fig. 4, at $Q^2 \approx 25\,\mathrm{GeV}^2$, which correpsonds to a value attainable in future experiments [6]. One can see that ratios calculated at the same $x_{\rm Bj}$ both in the numerator and in the denominator are dramatically different from the ones obtained with Eq. (11). Such a prescription could be also used to plot existing experimental data at $x_{\rm Bj} < 1$, in order to better clarify the role of nucleon binding in such a region (the *original EMC effect*).

To summarize, our results on cross section ratios for heavier to lighter nuclei at $x_{\rm Bj} > 1$ and Q^2 in the few GeV^2 region reflect the behavior of single cross sections and structure functions in the region of negative y_A (y). Contrary to what was observed in single cross sections, the contribution of two-body breakup channels is more

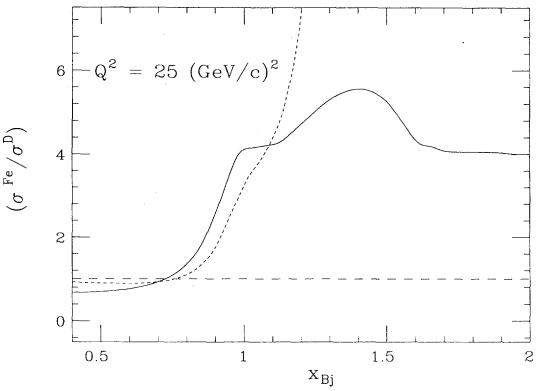

FIG. 4. Cross section ratios in the deep inelastic region. Results obtained by using the same $x_{\rm Bj}$ both in the numerator and in the denominator (short-dashed line) are compared with results obtained by using the prescription in Eq. (11) (full line).

visible in ratios, in the form of a bump centered around $x_{\rm Bj} \approx 1.2 - 1.3$ for all nuclei, and extending up to $x_{\rm Bj} \approx 1.4$. Unravelling direct information on few-nucleon correlations or other mechanisms such as multi-quark clusters is therefore difficult in such a region. The whole description of nucleon dynamics effects on inclusive ratios should be anyhow reexamined by properly choosing variables which would allow the probing of similar components of the nucleon spectral function in the heavier and lighter nuclei, respectively. Such an approach can be more fruitfully extended at higher Q^2 where FSI effects are most likely to be ignored.

I would like to thank J. McCarthy and D. Day for their warm hospitality at the Institute of Nuclear and Particle Physics in Charlottesville. In addition I thank D. Day and O. Benhar for useful discussions, P. Bosted for communicating his results prior to publication, and the Organizers of the "Workshop on the European Electron Facility" (Clermont-Ferrand) where the manuscript was completed. Finally I thank P.Q. Hung for his continuous encouragement and for reading the manuscript.

[1] European Muon Collaboration, J.J. Aubert *et al.*, Phys. Lett. **123B**, 275 (1983); R.G. Arnold *et al.*, Phys. Rev. Lett. **52**, 727 (1984).
[2] P. Bosted *et al.*, Report No. SLAC-PUB-5840, submitted to Phys. Rev. D.
[3] D.B. Day, Nucl. Phys. **A478**, 397c (1988).
[4] J.P. Vary, Nucl. Phys. **A418**, 195c (1984); J.P. Vary and A. Harindranath, in *The Three-Body Force in the Three-Nucleon System*, edited by B.L. Berman and B.F.Gibson, Lecture Notes in Physics 260 (Springer-Verlag, Berlin, 1986), p. 422.
[5] L.L. Frankfurt and M.I. Strikman, in *Modern Topics in Electron Scattering*, edited by B. Frois and I. Sick (World Scientific, Singapore, 1991), p. 645.
[6] E. Beise *et al.*, CEBAF Proposal PR-89-008 (1989); R.G. Arnold *et al.*, Report No. SLAC LOI (1991); A. Boudard *et al.*, Proposal for the European Electron Facility (1993).
[7] P.C. Tiemeijer and J.A. Tjon, Phys. Rev. C **42**, 599 (1990).
[8] F. Gross and S. Liuti, Phys. Rev. C **45**,1374 (1992).
[9] T. de Forest, Nucl. Phys. **A392**, 232 (1982).
[10] A. Bodek and J.L. Ritchie, Phys. Rev. D **23**, 1070 (1981).
[11] L.L. Frankfurt and M.I. Strikman, Phys. Rep. **160**, 235 (1988).
[12] C. Ciofi degli Atti, D.B. Day, and S. Liuti, Phys. Rev. C **46**, 1045 (1992).
[13] O. Benhar, A. Fabrocini, and S. Fantoni, Nucl. Phys. **A505**, 267 (1989).
[14] (a) C. Ciofi degli Atti and S. Liuti, Phys. Lett. B **225**, 215 (1988); Nucl. Phys. **A532**, 235c (1991); Phys. Rev. C **44**, R1269 (1991); (b) C. Ciofi degli Atti, S. Liuti, and S. Simula, Phys. Rev. C **41**, R2747 (1990).
[15] S. Pieper, R. Wiringa, and V. R. Pandharipande, Phys. Rev. C **46**, 1753 (1992).
[16] G.B. West, Phys. Rep. **18**, 263 (1975).
[17] E. Pace and G. Salmé, Phys.Lett. **110B**, 411 (1982).
[18] X. Ji and B. Filippone, Phys. Rev. C **42**, R2279 (1990).
[19] O. Benhar and S. Liuti, in preparation.
[20] L.S. Celenza, A. Rosenthal, and C.M. Shakin, Phys. Rev. C **31**, 232 (1985).